HTD-Vol. 203, Developments in Radiative Heat Transfer
ASME 1992

DIMENSIONALITY ISSUES IN MODELING WITH THE DISCRETE-ORDINATES METHOD

A. Sánchez A.
Escuela de Ingeniería Mecánica
Universidad de los Andes
Mérida, Venezuela

T. F. Smith and W. F. Krajewski
Department of Mechanical Engineering
University of Iowa
Iowa City, Iowa

ABSTRACT

In this paper, a simple method is presented to allow for the modeling of 1-, 2- and/or 3-D geometries by means of a single discrete-ordinates algorithm. The full three-dimensional effects that might exist, due to the presence of a collimated source and/or a sensor, are retained and, therefore, no further treatment of the intensity field is needed. Three examples are provided to illustrate and to validate the general applicability, accuracy, and computational efficiency of the technique. These examples include 1-, 2- and 3-D Cartesian geometries, both small and very large optical thicknesses, spectral media, spectral boundaries, and different relative settings of collimated sources and sensor line-of-sight. Comparisons with more traditional approaches to the lower dimensionality problem are presented to exemplify the advantages of the proposed method.

NOMENCLATURE

a	absorption coefficient, m^{-1}
b_n	coefficients for series expansion in Legendre polynomials of order n.
f_d	fraction of the reflectance that is diffuse
F	total number of points on a given level
I	radiation intensity, W/m^2-sr-μm
k	moment (0,1,2,...)
K	total number of directions in a quadrature of order N
L	length, m
M_1	higher degree of P_n in series expansion of Φ_{ij}
n(r)	particle size distribution, cm^{-3}-μm^{-1}
N	order of quadrature
P_n	Legendre polynomial of order n
$\vec{q}_r$	radiant flux vector, W/m^2
s	scattering coefficient, m^{-1}
S	source function term, W/m^3-sr-μm
S_1, S_2, S_3	thermal, scattering, and collimated source terms in Eq.(6), W/m^3-sr-μm
T	temperature, K
w_j	angular quadrature weight for direction j
w^*	added weight of all points on a given level
W	total number of wavelength bands
x, y, z	coordinates, m
Δx, Δy, Δz	differential lengths in x, y, and z directions, m
α	finite-difference weighting factor
β	extinction coefficient, (a+s), m^{-1}
γ	cosine of the angle between I and the z axis
δ	cosine of the angle between I and the y axis
δ'	Dirac-δ function
ε	surface emittance
ζ	line-of-sight distance, m
η	any direction cosine (μ, δ, or γ)
θ	polar angle, rad
θ_{ij}	scattering angle between directions i and j, rad.
κ	surface transmittance
λ	wavelength, μm
μ	cosine of the angle between I and the x axis
τ	optical thickness, βL
Φ	phase function for scattering
Φ	renormalized phase function defined by Eq. (16)
ϕ	azimuthal angle, rad
ψ	surface reflectance
ω_o	scattering albedo, s/β
Ω	cosine of angle between a discrete direction and normal to a surface

Subscripts

b	blackbody
ba	background
c	parallel beam
d	sensor
g	gas
i, j	i and j directions
k	any surface
m	mirroring direction
t	total
x, y, z	directions
λ	monochromatic

Superscripts

+	from boundary toward medium
-	from medium toward boundary
o	from outside toward the enclosure
p	average over the control volume
xe,ye,ze	end faces in x, y, and z directions
xr,yr,zr	reference faces in x, y, and z directions

INTRODUCTION

The discrete-ordinates method has been successfully applied to the solution of 1-, 2-, and 3-D radiative transfer problems in Cartesian coordinates. Specific versions of the discrete-ordinates method have been developed to take advantage of the symmetry and invariance related to each level of dimensionality. These specific models fail to retain, in 1- and 2-D applications, the 3-D effects implied by the presence of incident collimated sources and/or detecting sensors at locations that are outside the planes of symmetry. As a consequence of this, most applications found in the literature, limit parallel beam radiation and intensity output to a sensor to zero azimuthal angles (Kim and Lee, 1989) or a further treatment of the intensity field –normally a Fourier series expansion– is required in order to reach the desired solution (Stamnes, et al., 1988).

A higher dimensionality (3-D) discrete-ordinates model has been used in a few occasions to solve lower dimensionality (1- or 2-D) problems. In these few instances, the aspect ratio of the numerical domain is modified to imply "infinite" length(s), the boundaries in the "infinite(s)" direction(s) are modeled as specular boundaries, or the boundary conditions in the "infinite(s)" direction(s) are assumed periodic. These approaches to the lower dimensionality problem are, in general, inexact and computationally expensive and even prohibitive for large optical thicknesses.

In the literature, only one application could be found (Fiveland and Jamaluddin, 1991) where a discrete-ordinates code (3-D) was used in the solution of a problem of lesser dimensionality (1-D). The methodology used in that application consisted, basically, of using a very large aspect ratio in the "infinite" direction. This classical approach, although possible, is not practical in optically thick problems where a very large number of control volumes, and, therefore, computer memory, would be required. Because of this and other disadvantages of the method (ray or end effects), an alternative solution, based on the mirror technique (periodic or symmetric boundaries), was introduced by Sánchez, et al., 1991.

After each iteration, the discrete-ordinates method gives (without extra computations) the intensity field. A "mirror technique" can, therefore, be applied to the direction (2-D) or directions (1-D) of "infinite" length making the boundaries in these directions behave as periodic boundaries. This means, in practical terms, that the intensities going out of a surface (for a given iteration) are placed as intensities coming into the opposite wall (boundary condition for the next iteration) for the direction being modeled. In this iterative procedure, the side walls are considered transparent. It can be seen that, in the mirror technique, the aspect ratio is irrelevant and that no especial consideration about the side walls is needed. Although the mirror approach was a step in the right direction, the slow rate of convergency of the method greatly undermines its practical applicability.

The two techniques or approaches (mirror and classical) to the lesser dimensionality problem mentioned, fail to recognize the simple solution offered by the discrete-ordinates formulation. An examination of the derivation of the discretized equations that constitute the discrete-ordinates method reveals that the degree of dimensionality is dictated by the presence of the direction cosines and the scattering phase function. The description, formulation, and testing of a simple procedure (shortcut approach) allowing for the use of the same 3-D code, with the same quadrature set, and without modifications for the solution of 1-, 2-, and 3-D problems (which could include collimated sources and detecting sensors at any desired angle) is one of the goals of this work. This capability would allow for the comparison and possible parameterization of predictions obtained using different dimensionalities in the solution of a given problem. These comparisons and parameterizations would be free from the influences of different quadratures or solution procedures.

ANALYSIS

Geometry

The complete 3-D system is shown in Fig. 1. The media, which can absorb, emit, and anisotropically scatter radiation, is contained in a parallelepiped whose walls can be, in any combination, opaque or transparent. The direction of incidence of the parallel beam as well as the direction of the sensed intensity are arbitrary for both polar and azimuthal angles.

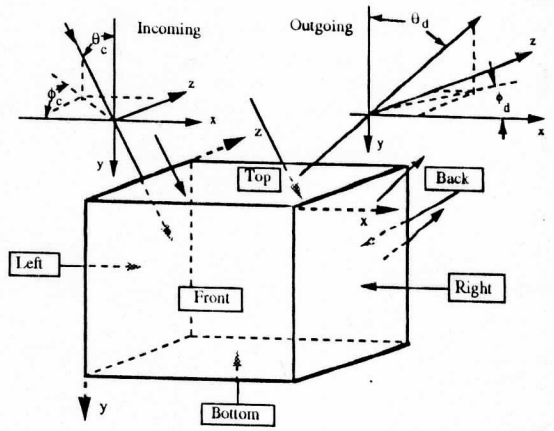

Fig. 1 General 3-D geometry

General 3-D formulation

Several formulations of the discrete-ordinates method are available (Carlson and Lathrop, 1968; Hyde and Truelove, 1977; Fiveland, 1988; Fiveland and Jamaluddin, 1991; Kim and Lee, 1989; Sánchez, 1991). The present formulation has been extracted from Sánchez (1991). The meanings of all the terms and variables are provided in the nomenclature and explained, in detail, in the mentioned reference.

The full intensity is written as

$$I_{i\lambda}(\tau_\lambda) = I_\lambda(\tau_\lambda) + \delta'(\mu - \mu_c)\,\delta'(\delta - \delta_c)\,\delta'(\gamma - \gamma_c)\,I_{c\lambda}(\tau_\lambda) \qquad (1)$$

The first and second terms on the right hand side of Eq. (1) represent the scattered intensity and the direct intensity.

The direct intensity is

$$I_{c\lambda}(\tau_\lambda) = I_{c\lambda}(0)\exp(-\tau_\lambda) \qquad (2)$$

The numerical implementation of this direct intensity is not obvious, and the reader is referred to Sánchez (1991) for a complete description this procedure.

In terms of the reference intensities, the average scattered intensity for each control volume is given by

$$I_i^P = \frac{\frac{|\mu_i|}{\Delta x} I_{xr}^i + \frac{|\delta_i|}{\Delta y} I_{yr}^i + \frac{|\gamma_i|}{\Delta z} I_{zr}^i + \alpha S}{\left(\frac{|\mu_i|}{\Delta x} + \frac{|\delta_i|}{\Delta y} + \frac{|\gamma_i|}{\Delta z}\right) + \alpha\beta} \qquad (3)$$

The intensity arriving at the end-faces (which becomes the reference for the neighboring control volumes) are recovered from

$$I_{xe}^i = \left[I_i^P + (\alpha - 1)\,I_{xr}^i\right]/\alpha \qquad (4)$$

The finite-difference weighting factor is unity. Expressions for

y and z are written by interchanging x with y and z. The source term is

$$S = S_{1i}^P + S_{2i}^P + S_{3i}^P \tag{5}$$

where

$$S_{1i}^P = a\, I_b(\zeta, T^P) \tag{6a}$$

$$S_{2i}^P = \frac{s}{4\pi} \sum_j^K w_j\, I_j^P\, \Phi_{ij} \tag{6b}$$

$$S_{3i}^P = \frac{s}{4\pi}\, I_c^P\, \Phi_{ic} \tag{6c}$$

The boundary conditions for Eq. (3) are

$$I^+ = \varepsilon\, I_b^+ + \kappa\, [I_{ba}^o + \delta(\mu_i - \mu_c)\, \delta(\delta_i - \delta_c)\, \delta(\gamma_i - \gamma_c)\, I_c^o] + \frac{\Psi}{\pi} f_d\, [I_c^- + \sum_{\Omega_i<0} I^-\, \Omega_i] + \Psi(1-f_d)\, I_m^- \tag{7}$$

The divergence of the radiative flux vector is

$$\nabla \cdot \vec{q}_r = \sum_{n\lambda=1}^{W} \left[a \left(4\pi\, I_b^P - \sum_{j=1}^{K} w_j\, I_{ij} - I_c^P \right) \right]_{n\lambda} \tag{8}$$

The heat flux at any given surface k

$$q_k = \sum_{n\lambda=1}^{W} \left(I_c^-\, \eta_c + \sum_{j=1}^{K} w_j\, \eta_j\, I_{ij} \right)_{n\lambda} \tag{9}$$

With the radiative transfer equations discretized, it is only a matter of solving for the radiant intensities, divergence of the radiative heat flux, and surface heat fluxes given the boundary conditions and radiative properties.

The shortcut approach

An examination of the derivation of Eq. (3) (Sánchez, 1991) reveals that the degree of dimensionality is dictated by the presence of the direction cosines and the scattering phase function. The shortcut approach to simulate lower dimensionalities by means of a general 3-D code is as follows:

1) The quadrature set is selected (3-D). Of the many possibilities (Fiveland, 1991), the level sequential-odd quadrature was chosen. In order to comply with the restrictions related to symmetry and moments matching, the quadrature set has to satisfy three equations

$$\mu_i^2 = \mu_1^2 + 2\, \frac{(i-1)}{(N-2)}\, (1 - 3\mu_1^2) \quad ; \quad \text{for } i = 1,2...N/2 \tag{10}$$

$$\sum_{j=1}^{N/2} w_j'\, m_j^k = \frac{\pi}{2(k+1)} \tag{11}$$

$$\sum_{m=1}^{F} w_m = w_j' \tag{12}$$

where F = N/2 - j + 1

2) The phase function is calculated for all pairs of directions (including, if present, beam and sensor). The phase function for a single particle is calculated from the scattering of a sphere and the integrated phase function for polydispersions is evaluated from standard formulas (Sánchez, et al., 1991). The function obtained in this manner is expressed in terms of Legendre polynomials according to

$$\Phi_{ij} = \sum_{n=0}^{M_1} (2n+1)\, b_n\, P_n(\cos(\theta_{ij})) \tag{13}$$

Having selected the desired order (N) of the quadrature set the cosine of the angle between all pair of discrete directions is found from

$$\cos(\theta_{ij}) = \mu_i\mu_j + \delta_i\delta_j + \gamma_i\gamma_j \tag{14}$$

and implemented in Eq. (13) in order to find Φ_{ij} for any ij combination. The phase function obtained in this way is then renormalized according to

$$\dot{\Phi}_{ij} = \Phi_{ij} \Big/ \frac{1}{4\pi} \sum_{i=1}^{K} \Phi_{ij}\, w_i \tag{15}$$

This result forms a database to be used with Eq. (3). The database of phase function values preserves the implicit 3-D information due to beam and/or sensor.

3) The direction cosines in the direction (2-D) or directions (1-D) of "infinite" length are set to zero. For 2-D problems (x and y), this results in

$$\gamma_i = 0.0 \qquad \forall_i \tag{16}$$

For 1-D problems (y), the following equation is added to Eq. (16)

$$\mu_i = 0.0 \qquad \forall_i \tag{17}$$

4) The resulting system of governing equations is solved as usual.

The shortcut approach has been successfully incorporated into an existing, and tested, 3-D discrete-ordinates code (Sánchez, et al., 1991). The resulting algorithm, named ANDISORD4 (Sánchez, 1991), allows the user to select and solve 1-, 2-, or 3-D geometries independently of the boundary conditions and independently of the presence or not of collimated sources and/or sensors. ANDISORD4 has been used in the solution of the examples that follow.

RESULTS AND DISCUSSION

Test 1

Edwards and Nelson (1962), Siegel and Howell (1972), and Fiveland and Jamaluddin (1991) predicted radiative transfer between two parallel, nongray plates spaced 2.54 cm as shown in Fig. 2. The hot and cold plates are maintained at 1111 K and 556 K. Pure CO_2 at a pressure of 1.013 MPa and a temperature of 556 K is between the plates. Spectral wall emittances (ε_w) and gas absorption coefficients (a_g) cited in Table 1 were taken from Fiveland and Jamaluddin (1991), and are based on the calculations in Siegel and Howell (1972). Edwards and Nelson (1962) used a different band model which accounts for the difference between their results and those of Siegel and Howell (1972). The results from Edwards and Nelson (1962), therefore, are given as a reference only. Comparisons are made against the work of Siegel and Howell (1972). Three different approaches to the numerical solution

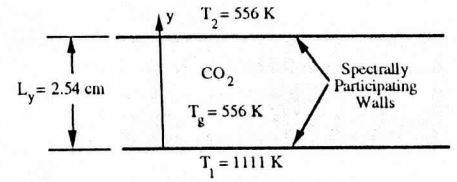

Fig. 2 Geometry for Test 1

Table 1 Spectral data for Test 1

Wavenumber, cm^{-1} Min		Max	ε_w	a_g m^{-1}
0	—	555	0.37	0.0
555	—	779	0.26	49.05
779	—	849	0.32	0.0
849	—	1013	0.37	1.348
1013	—	1141	0.46	1.743
1141	—	2221	0.45	0.0
2221	—	2430	0.65	∞
2430	—	3573	0.61	0.0
3573	—	3750	0.69	∞
3750	—	∞	0.73	0.0

of this 1-D problem by means of the 3-D discrete ordinates code are presented next.

The classical approach. While Edwards and Nelson (1962) and Siegel and Howell (1981) used analytical approaches to solve the problem, Fiveland and Jamaluddin (1991) used a 3-D discrete-ordinates model to simulate the 1-D geometry. To model the 1-D geometry, Fiveland and Jamaluddin applied a $4 \times 4 \times 4$ computational grid to a 3-D control volume with an aspect ratio of 1:24:24 ($L_x/L_y = 24$, and $L_x/L_z = 24$). The end walls were assumed to behave as cold, diffusely reflecting surfaces (with very low emittance, $\varepsilon = 0.0001$). Using the same modeling approach, ANDISORD4 was applied to a $5 \times 5 \times 5$ computational grid (this grid gives the heat flux at the central region of the plates and was considered to be more appropriate than the $4 \times 4 \times 4$ grid). Predicted local and averaged heat fluxes are shown in Fig. 3.

Fiveland and Jamaluddin (1991) suggested, based on the average heat fluxes presented in Table 2, that their modeling of the 1-D geometry by means of the 3-D code was correct, and that the non-uniform profiles shown in Fig. 3 are a consequence of end effects, which could be improved by increasing L_x/L_y and L_x/L_z. These ideas would seem to indicate that the predictions of ANDISORD4, although locally very different from those of Fiveland and Jamaluddin (1991) are also correct. A closer look into the problem is in order.

Modeling the side walls as diffusely reflecting walls (producing the results shown in Fig. 3 and Table 2) should produce averaged heat fluxes on the receiving (cold) wall that are smaller than those for the parallel plate geometry. The reason being that part of the energy from the hot wall reaching the side walls (which in the 1-D geometry would arrive at the cold wall) will be re-directed back to the emitting wall resulting in a net decrease in the total energy arriving at the receiving wall. These averaged heat fluxes, therefore, do not provide enough information about the goodness of the modeling.

When a 1-D geometry is modeled by a 3-D control volume with a large aspect ratio (classical approach), the heat flux at the center of the larger surfaces (and not the heat flux averaged over those surfaces) would be the closest indication of the heat flux for the modeled 1-D geometry. At this central location, end effects are minimized. Table 3 presents the heat flux at the central location of the receiving surface as predicted by the different methods. Table 3 indicates good agreement between ANDISORD4 and results from Siegel and Howell

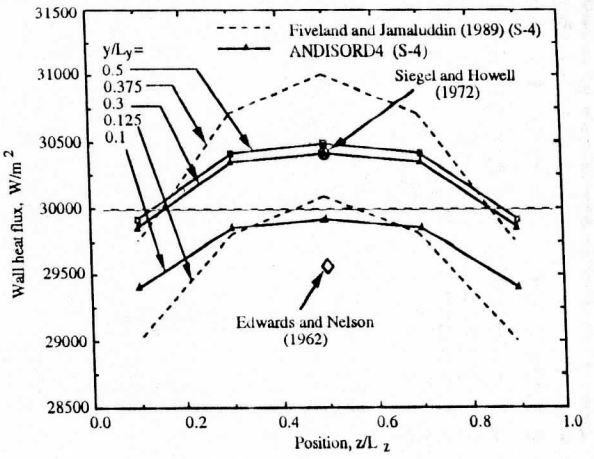

Fig. 3 Local wall heat fluxes to receiving wall

Table 2 Averaged heat flux on receiving wall

Siegel and Howell, (1981)	30417.00 W/m^2
Fiveland and Jamaluddin1 (1991)	29991.00 W/m^2
ANDISORD4	29991.75 W/m^2
Edwards and Nelson (1962)	29562.00 W/m^2

Table 3 Heat flux at the center of receiving wall

Fiveland and Jamaluddin (1991)	>31000.00 W/m^2
ANDISORD4	30483.38 W/m^2
Siegel and Howell (1981)	30417.00 W/m^2
Edwards and Nelson (1962)	29562.00 W/m^2

(1981) (the spectral properties used in both studies are the same). Fiveland and Jamaluddin (1991) on the other hand, clearly overestimate the heat flux.

The mirror approach. When the mirror technique (Sánchez, et al., 1991) is applied to the test problem, ANDISORD4 produces the results shown in Fig. 4 and Table 4. The results do not change when the aspect ratio is changed from 1:1:1 to 1:24:24. The uniform heat flux depicted in Fig. 4 indicates the excellent 1-D simulation provided by the mirror technique. The numerical values presented in Table 4 indicate that ANDISORD4 over predicts the heat flux of Siegel and Howell (1981) by less than 1percent.

The shortcut approach. It was explained in the previously outlined procedure that the 3-D discrete-ordinates formulation of the equation of transfer offers the possibility of simulating lower order dimensionalities by the simple and expeditious procedure of setting to zero the direction cosines in the infinite ordinate directions. For 1-D modeling, in particular, the direction cosines with z and x (γ_i and μ_i) are set to zero for the discrete directions. When this method is applied, the results presented in Table 5 are obtained. As in the mirror case, the error in the computed heat flux is less than 1 percent and the heat flux profiles are uniform, with a representation similar to that in Fig. 4.

Remarks. From the preceding discussion, it can be concluded that:

1) When the 1-D geometry is modeled with the classical approach, the local heat flux at the center of the receiving plate (evaluated with ANDISORD4) correctly estimates,

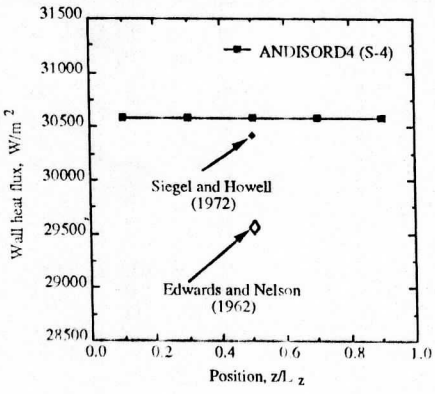

Fig. 4 Local wall heat fluxes by mirror approach

Table 4 Heat flux predicted by mirror approach

ANDISORD4	30576.84 W/m²
Siegel and Howell (1981)	30417.00 W/m²
Edwards and Nelson, (1962)	29562.00 W/m²

Table 5 Heat flux for shortcut approach

ANDISORD4	30572.24 W/m²
Siegel and Howell, (1981)	30417.00 W/m²
Edwards and Nelson (1962)	29562.00 W/m²

on the same plate, the averaged heat flux.

2) Most of the energy transfer takes place in the transparent bands. Siegel and Howell (1981) report 97.46 percent of the total heat exchange as taking place in these bands. Computations using ANDISORD4 yielded a value of 97.59 percent. Discrete-ordinate codes are known to have difficulties in situations involving transparent media. These difficulties, known as ray or end effects, are mainly due to numerical diffusion as a consequence of coarse discretization for the problem at hand and become important in 2-D and 3-D geometries (Gerstl and Zardecki, 1985; Sánchez and Smith, 1992). The applicability of the classical approach in situations involving large optical thickness is thus questionable.
3) When properly modeled (mirror or shortcut methods), ANDISORD4 gives the correct answer to the 1-D problem under consideration (Fig. 4 and Tables 4 and 5).
4) Although the final results are equivalent to those obtained with the mirror technique, the "shortcut" approach is numerically more efficient than the mirror method. On a personal computer, the shortcut approach needed 125 s to obtain the solution given in Table 5 while the mirror technique needed 916 s to solve the same problem (Table 4). This numerical efficiency and accuracy, together with the fact that no modification of the original code is required, make the shortcut approach superior to the classical and the mirror methods.

TEST 2

The geometry and the conditions for the problem modeled in this test are those shown in Fig. 5. The medium scatters radiation isotropically and is cold, gray, and contained in a parallelepiped whose top wall is transparent; the other enclosure walls are opaque and black, and the length of the domain in the z direction is infinite.

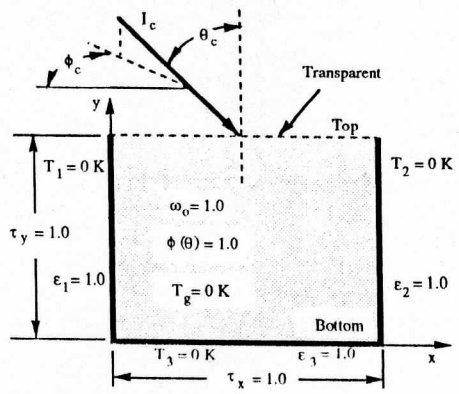

Fig. 5 Geometry for Test 2

The classical approach. Starting with a cubical enclosure of unit optical thickness ($\tau_x = \tau_y = \tau_z = 1$), the optical thickness in the z direction is increased in order to approach, at $\tau_z/2$, the 2-D solution of Tan and Howell (1990). Results for five different values of τ_z are presented in Fig. 6, where the dimensionless heat fluxes are defined as the net fluxes divided by the heat flux at the top wall due to the parallel beam. The 2-D results, including shadowing effects, are essentially represented by those for $\tau_z = 5$.

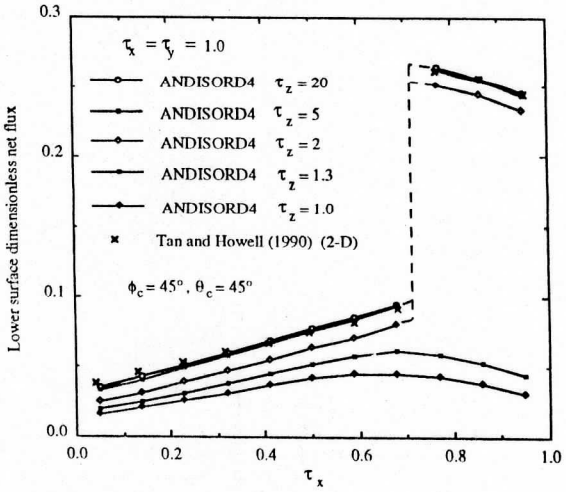

Fig. 6 Classical approach: heat fluxes at $z = L_z/2$

The mirror and shortcut approaches. Figure 7 shows the results obtained when either the mirror or the shortcut approaches are applied. The results obtained in both cases show excellent agreement with Tan and Howell (1990). The shadowing effects are also very well represented. Although the numerical results obtained with the two approaches are indistinguishable, the computational time needed in each case is very different. The mirror approach required 308 s (wall clock time) to solve the problem while the shortcut approach needed only 70 s to give the same results.

Remarks. The classical approach, applied over an $11 \times 11 \times 11$ grid mesh, and with $\tau_z = 20$, required 780 s of wall clock time to solve the problem. The mirror technique needed an $11 \times 11 \times 1$ grid mesh and 308 s to achieve the same results. Finally, the shortcut approach, applied over an 11×11 grid, demanded only 70 s of wall clock time to converge to the solution shown in Fig. 7.

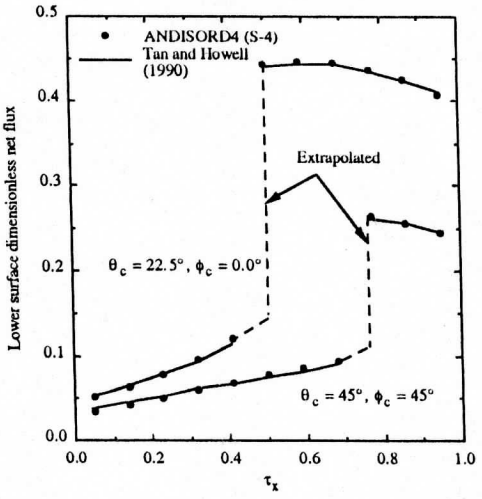

Fig. 7 Mirror or shortcut approach for Test 2

Test 3

The object of this test, proposed by the Radiation Commission (Lenoble, 1985), concerns a thicker atmosphere (approximately a 4 km thick cloud) in the plane-parallel setting depicted in Fig. 8. The computations are carried out for λ = 0.7 μm assigning a refractive index for water of 1.33. For the case being solved here, a representative output angle of θ_d = 53.13 deg (δ_d = 0.6) is selected. A polydispersion of type C1 is reported to have a drop size distribution resembling that found in real clouds. The C1 drop size distribution has the form (Deirmendjian, 1964; Lenoble, 1985):

$$n(r) = 2.373\, r^6 \exp(-1.5r) \qquad (19)$$

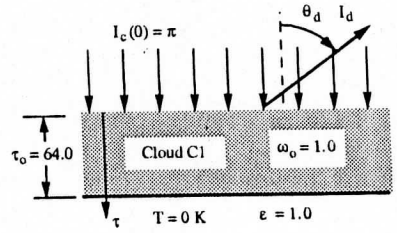

Fig. 8 Geometry for Test 3

Radiative properties. To obtain an accurate solution for such a thick atmosphere, many layers would be required in the computational domain. Furthermore, a highly anisotropic scattering phase function is expected, due to the relative size of the wavelength under consideration and the range of the particle size in the polydispersion ($0.1 \le r \le 15$ μm). This is a typical situation where the δ-M scaling (Wiscombe, 1977) should be used.

To evaluate the radiative properties, it is necessary to (Sánchez, 1991) calculate, from the theory for the scattering of spherical particles (Dave, 1964; Bohren and Huffman, 1983), the extinction and scattering cross-sections as well as the phase function based on the wavelength, the refractive index, and the particle radius; obtain the radiative properties for the

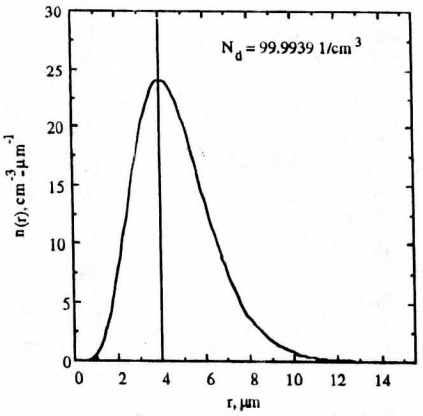

Fig. 9 Drop size distribution for cloud C1

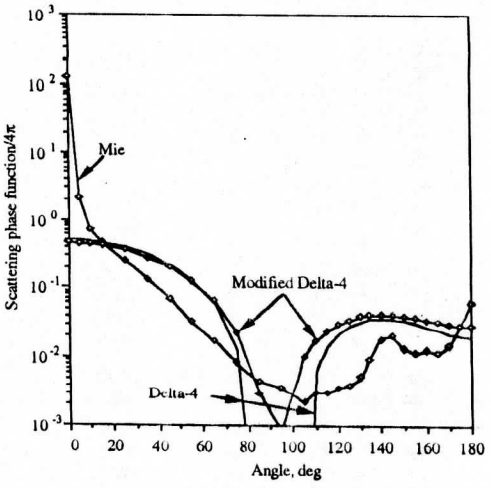

Fig. 10 Phase function for cloud C1, λ = 0.7 μm

polydispersion; expand the phase function in a series of Legendre polynomials; apply the δ-M scaling to the phase function to find the transformed properties; and apply the modified δ-M scaling to eliminate negative values from the phase function. The drop size distribution and the calculated phase functions (Mie, δ-M, and modified δ-M) are shown in Figs. 9 and 10.

In Fig. 9, the computed values for drop number density (N_d = 99.99 cm^{-3}) and the mode radius (r_c = 4 μm) are also indicated. Figure 10 shows good agreement between the computed spherical particle phase function and the table of values (at 1° spacing) provided by Lenoble. The negative values (not shown in Fig. 10) of the transformed δ-4 phase function are corrected by the modified δ-4 phase function.

One of the advantages of the δ-M scaling is the transformation of the domain from the original optically thick domain to a new, thinner one. Values of the scattering and extinction coefficients at each stage of the calculation are tabulated in Table 6. From this information, the optical thickness is reduced to 1/3 of its original value.

Classical and mirror approaches. The large optical thickness characterizing this problem renders the classical and mirror approaches useless due to their particular shortcomings. The grid size required (and consequently the memory needed) by the classical approach, even after the δ-M scaling of the domain, makes this technique impractical (even impossible) for

Table 6 Scaling of the optical thickness

Type of Calculations	β_λ, 1/km	τ_λ
Mie	16.757	64.0
δ-4	7.004	26.75
Modified δ-4	5.594	21.75

this type of application. The mirror approach, on the other hand, can require thousands of iterations until convergence is achieved. Lack of computer memory in the personal computer used for this study prevented the application of the classical approach to the problem at hand. After several hours of slowly converging computations, the mirror approach was considered clearly impractical, and the computational process was aborted.

Shortcut approach. ANDISORD4 was run with a S-8 (40 streams up and 40 streams down) quadrature set and 10, 20, and 30 layers. The worst results ($I_d(0)$ and $q_{net}(0)$ for intensity toward sensor and net flux, respectively) always take place at the top surface. When the number of layers is increased from 20 to 30, the intensity toward the sensor (at $\tau = 0$) increased by less than 0.4 percent while the net flux decreased by less than 1.5 percent. From this information (Table 7), it can be concluded that with 30 layers (requiring approximately 45 min of wall clock time) the results are practically converged.

Table 7 Influence of number of layers

Layers	$I_d(0)$	Change	$q_{net}(0)$	Change
10	0.8377		0.5207	
20	0.8533	-1.83 %	0.4867	6.99 %
30	0.8566	-0.39 %	0.4799	1.42 %

It is reported by Lenoble (1985) that different treatment was given, by different authors, to the phase function and that the δ-M scaling technique was used by some of them. Tables 8 and 9 contain, for comparison, the results obtained in this study (with 30 layers) and some of the results from other methods (using specialized 1-D codes) reported by Lenoble (1985).

Remarks The results obtained by means of the shortcut approach, are in good agreement with the results provided by other methods. From the results presented in Tables 7 to 9, it is seen that even the 10 layer approximation could have been used with approximately the same degree of uncertainty.

CONCLUSIONS

There is a wide variety of specialized 1-D and 2-D models available in the literature, many of them excellent, that can handle practically any degree of difficulty. These specialized models are conceived to take maximum advantage of the possible symmetry that might exist in the numerical domain. The presence of a collimated source or a detecting sensor, however, introduces 3-D effects in the radiation field that seriously jeopardize the applicability of these models. As a possible solution to this problem, an efficient technique (the shortcut approach) to the lesser dimensionality problem by means of a full 3-D formulation is presented and tested.

A complete set of equations allowing for the solution of radiative transfer problems in 3-D domains by means of the discrete-ordinates method is summarized. For a given set of boundary and media conditions, the solution of these equations provides a discrete number of intensities containing enough information to allow for the complete description of the 3-D

Table 8 Intensity toward the sensor for Cloud C1, $\omega_0 = 1.0$

Method	Intensity toward sensor ($\delta_d = 0.6$)				
	$\tau = 0$	$\tau = 3.2$	$\tau = 12.8$	$\tau = 32$	$\tau = 48$
Spherical harmonics.D	0.825	0.978	0.902	0.570	0.291
Spherical harmonics.K	0.826	0.979	0.902	0.570	0.292
Finite difference.	0.805	—	—	—	—
Monte Carlo.M.K	0.788	0.816	0.851	0.449	0.307
Monte Carlo.M.K	0.829	—	—	—	—
Asymptotic	0.821	—	0.901	0.568	0.292
ANDISORD4	0.857	0.977	0.908	0.575	0.294

xx interpolated value (underlined)

Table 9 Fluxes: Cloud C1, ω_0=1.0

Method	Net flux (direct + diffuse)					
	$\tau = 0$	$\tau = 3.2$	$\tau = 12.8$	$\tau = 32$	$\tau = 48$	$\tau = 64$
Spherical harmonics. D	0.4828	0.4826	0.4825	0.4823	0.4822	0.4821
Spherical harmonics.K	—	0.4806	0.4806	0.4806	0.4806	0.4806
Finite difference.	0.4811	0.4811	0.4811	0.4811	0.4811	0.4811
Monte Carlo.Mc.K	0.4856	—	—	—	—	0.4856
Asymptotic	0.4900	—	0.4950	0.4950	0.4950	0.4950
Discrete ordinates. L	0.4630	—	—	—	—	0.4630
Doubling	0.4796	0.4796	0.4796	0.4796	0.4796	0.4796
Eddington W.	0.4731	0.4731	0.4731	0.4731	0.4731	0.4731
Eddington + similarity	0.4756	0.4756	0.4756	0.4756	0.4756	0.4756
Delta Eddington B.	0.4759	0.4759	0.4759	0.4759	0.4759	0.4759
Standard Two streams	0.6703	0.6703	0.6703	0.6703	0.6703	0.6703
Exponential kernel	0.4759	0.4759	0.4759	0.4759	0.4759	0.4759
ANDISORD4	0.480	0.480	0.480	0.480	0.479	0.479

xx interpolated value (underlined)

radiation field and for the evaluation of derived quantities (fluxes).

The simplicity and power of the discrete-ordinates method is evidenced by verifying the possibility of modeling 1-D and 2-D problems (while preserving the description of the 3-D radiation field) by the straightforward and expeditious procedure of setting to zero, after the evaluation of the full scattering phase function, the direction cosine(s) corresponding to the "infinite" length(s) of the domain. This shortcut approach to the lesser dimensionality issue is tested and compared with two existing techniques: the classical and the mirror approaches. It is possible to conclude, from the examples presented, that the shortcut approach allows for the solution of 1-D, 2-D, and 3-D problems by means of a single computer algorithm. Of particular importance is the fact that in all three dimensionalities, parallel beam and detectors can be included without any alteration of the code.

When compared with the classical and the mirror approaches, the shortcut approach is noticeably faster and less memory demanding. In optically thick applications (Test 3),

the shortcut approach can be the only viable alternative to the lesser dimensionality problem. Further, end or ray effects, which can be important in the classical approach, are not a concern in either the mirror or the shortcut approaches.

The shortcut approach is an excellent choice for problems related to remote sensing applications and/or dimensional parameterization of results.

ACKNOWLEDGMENTS

The described investigations were partially supported by the grant NA89AA-D-AC195 from the National Oceanic and Atmospheric Administration: Global Change Program. The authors are thankful for this support. The first author would also like to acknowledge the financial support received from Universidad de los Andes and Fundación Gran Mariscal de Ayacucho, both from the Republic of Venezuela.

REFERENCES

Bohren, C. F. and Huffman, D. R., Absorption and Scattering of Light by Small Particles, John Wiley and Sons, New York, 1983.

Carlson, B. G. and Lathrop, K. D., 1968, "Transport Theory, The Method of Discrete-Ordinates," Computing Methods in Reactor Physics, Eds. H. Greenspan, C. N. Kelber, and D. Okrent, Gordon and Breach, New York, pp. 171-266.

Dave, J. V., Subroutines for Computing the Parameters of the Electromagnetic Radiation Scattered by a Sphere, Report No. 320-3237, IBM Scientific Center, Palo Alto, California, 1968.

Deirmendjian, D., 1964, "Scattering and Polarization Properties of Water Clouds and Hazes in the Visible and Infrared," Applied Optics, Vol. 3, No. 2, pp. 187-196.

Edwards, D. and Nelson, K., 1962, "Rapid Calculations of Radiant Energy Transfer Between Nongray Walls and Isothermal H_2O and CO_2 Gas," J. of Heat Transfer, Vol. 84, pp. 273-278.

Fiveland, W. A., 1988, "Three-Dimensional Radiative Heat Transfer Solutions by the Discrete-Ordinates Method," J. Thermophysics and Heat Transfer, Vol. 2, No. 4, pp. 309-316.

Fiveland, W. A., 1991, "The Selection of Discrete Ordinate Quadrature Sets for Anisotropic Scattering," Fundamentals of Radiation Heat Transfer, Eds. W. A. Fiveland, A. L. Crosbie, A. M. Smith, and T. F. Smith, ASME HTD-Vol. 160, pp. 89-96.

Fiveland, W. A. and Jamaluddin, A. S., 1991, "Three Dimensional Spectral Radiative Heat Transfer Solutions by The Discrete-Ordinates Method," J. Thermophysics and Heat Transfer, Vol 5, No. 3, pp. 335-339.

Gerstl, S. A. W. and Zardecki, A., 1985, "Discrete-Ordinates Finite-Element Method for Atmospheric Radiative Transfer and Remote Sensing," Applied Optics, Vol. 24, No. 1, pp. 81-93.

Hyde, D. J. and Truelove, J. S., 1977, The Discrete Ordinates Approximation for Multidimensional Radiant Heat Transfer in Furnaces, Report AERE-R 8502, AERE Harwell, Oxfordshire.

Kim, T. K. and Lee, H. S., 1989, "Radiative Transfer in Two-Dimensional Anisotropic Scattering Media with Collimated Incidence," J. Quant. Spectrosc. Radiat. Transfer, Vol. 42, No. 3, pp. 225-238.

Lenoble, J., 1985, Radiative Transfer in Scattering and Absorbing Atmospheres: Standard Computational Procedures, Deepack Publishing, Virginia.

Sánchez, A., 1991, "A General Purpose Radiative Transfer Model for Application to Remote Sensing in Multi-Dimensional Systems," Ph.D. Thesis, The University of Iowa, Iowa City, Iowa.

Sánchez, A., Smith, T. F., and Krajewski, W. F., 1991, "Three-Dimensional Radiative Heat Transfer in a Polydispersion with Collimated Incident Source," Fundamentals of Radiation Heat Transfer, Eds. W. A. Fiveland, A. L. Crosbie, A. M. Smith, and T. F. Smith, ASME HTD-Vol. 160, pp. 27-36.

Siegel, R. and Howell, J. R., 1981, Thermal Radiation Heat Transfer, Hemisphere Publishing Corporation, Washington.

Stamnes, K., Tsay, S.-C., Wiscombe, W., and Jayaweera, K., 1988, "Numerically Stable Algorithm for the Discrete-Ordinate-Method Radiative Transfer in Multiple Scattering and Emitting Layered Media," Applied Optics, Vol. 27, No. 12, pp. 2502-2509.

Tan, Z. and Howell, J. R., 1990, "Two-Dimensional Radiative Heat Transfer in an Absorbing, Emitting, and Linearly Anisotropic Scattering Medium Exposed to a Collimated Source," Radiation Heat Transfer: Fundamentals and Applications, Eds. T. F. Smith, M. F. Modest, A. M. Smith, and S. T. Thynell, ASME HTD-Vol. 137, pp. 101-116.

Wiscombe, W. J., 1977, "The Delta-M Method: Rapid yet Accurate Radiative Flux Calculations for Strongly Asymmetric Phase Functions," J. Atmospheric Sciences, Vol. 34, No. 9, pp. 1408-1442.